

## OPEN ACCESS

## EDITED BY

Ciriyam Jayaprakash,  
The Ohio State University, United States

## REVIEWED BY

Juan Carlos Yam-Puc,  
University of Cambridge, United Kingdom  
Alexander Thomas Stewart,  
University of Surrey, United Kingdom

## \*CORRESPONDENCE

Qiang Zhang  
[qiang.zhang@emory.edu](mailto:qiang.zhang@emory.edu)

RECEIVED 27 January 2024

ACCEPTED 14 May 2024

PUBLISHED 30 May 2024

## CITATION

Mu DP, Scharer CD, Kaminski NE and Zhang Q (2024) A multiscale spatial modeling framework for the germinal center response. *Front. Immunol.* 15:1377303.  
doi: 10.3389/fimmu.2024.1377303

## COPYRIGHT

© 2024 Mu, Scharer, Kaminski and Zhang. This is an open-access article distributed under the terms of the [Creative Commons Attribution License \(CC BY\)](#). The use, distribution or reproduction in other forums is permitted, provided the original author(s) and the copyright owner(s) are credited and that the original publication in this journal is cited, in accordance with accepted academic practice. No use, distribution or reproduction is permitted which does not comply with these terms.

# A multiscale spatial modeling framework for the germinal center response

Derek P. Mu<sup>1</sup>, Christopher D. Scharer<sup>2</sup>, Norbert E. Kaminski<sup>3</sup> and Qiang Zhang<sup>4\*</sup>

<sup>1</sup>Montgomery Blair High School, Silver Spring, MD, United States, <sup>2</sup>Department of Microbiology and Immunology, School of Medicine, Emory University, Atlanta, GA, United States, <sup>3</sup>Department of Pharmacology & Toxicology, Institute for Integrative Toxicology, Center for Research on Ingredient Safety, Michigan State University, East Lansing, MI, United States, <sup>4</sup>Gangarosa Department of Environmental Health, Rollins School of Public Health, Emory University, Atlanta, GA, United States

The germinal center response or reaction (GCR) is a hallmark event of adaptive humoral immunity. Unfolding in the B cell follicles of the secondary lymphoid organs, a GC culminates in the production of high-affinity antibody-secreting plasma cells along with memory B cells. By interacting with follicular dendritic cells (FDC) and T follicular helper (Tfh) cells, GC B cells exhibit complex spatiotemporal dynamics. Driving the B cell dynamics are the intracellular signal transduction and gene regulatory network that responds to cell surface signaling molecules, cytokines, and chemokines. As our knowledge of the GC continues to expand in depth and in scope, mathematical modeling has become an important tool to help disentangle the intricacy of the GCR and inform novel mechanistic and clinical insights. While the GC has been modeled at different granularities, a multiscale spatial simulation framework – integrating molecular, cellular, and tissue-level responses – is still rare. Here, we report our recent progress toward this end with a hybrid stochastic GC framework developed on the Cellular Potts Model-based CompuCell3D platform. Tellurium is used to simulate the B cell intracellular molecular network comprising NF-κB, FOXO1, MYC, AP4, CXCR4, and BLIMP1 that responds to B cell receptor (BCR) and CD40-mediated signaling. The molecular outputs of the network drive the spatiotemporal behaviors of B cells, including cyclic migration between the dark zone (DZ) and light zone (LZ) via chemotaxis; clonal proliferative bursts, somatic hypermutation, and DNA damage-induced apoptosis in the DZ; and positive selection, apoptosis via a death timer, and emergence of plasma cells in the LZ. Our simulations are able to recapitulate key molecular, cellular, and morphological GC events, including B cell population growth, affinity maturation, and clonal dominance. This novel modeling framework provides an open-source, customizable, and multiscale virtual GC simulation platform that enables qualitative and quantitative *in silico* investigations of a range of mechanistic and applied research questions on the adaptive humoral immune response in the future.

## KEYWORDS

B cells, germinal center, dark zone, light zone, affinity maturation, proliferative burst, chemotaxis

## 1 Introduction

The adaptive humoral immune response is a vital component of host defense, where B cells terminally differentiate into plasma cells (PCs) that secrete antibodies specifically recognizing and neutralizing the invading foreign antigens. The B cell responses can be broadly classified into two types: T cell-dependent and independent, depending on whether helper T (Th) cells are involved (1). In the T cell-independent response, naive B cells are activated directly via toll-like receptors (TLR) recognizing pathogen components such as lipopolysaccharide (LPS) or CpG DNA or via B cell receptors (BCR), without the assistance of Th cells (2, 3). The response is launched quickly and can occur within a few days of initial infection. Upon activation, B cells undergo clonal proliferation and differentiate into PCs, which secrete pentameric IgM molecules. While these antibodies provide initial protection, they are often polyclonal, not highly specific, and the IgM-secreting PCs are short-lived, thus unable to provide long-term immunity. In contrast, the T cell-dependent B cell response takes longer to develop, but through affinity maturation and class switch recombination (CSR) it can produce long-lived PCs that can provide life-long immunity with high-affinity IgG or other non-IgM antibody classes (4). Additionally, memory B cells are generated during the primary response, which can quickly launch a secondary antibody response upon subsequent exposure to the same antigens (5).

T cell-dependent B cell activation can take place either extrafollicularly, e.g., at the T-B border (6), or intrafollicularly in the germinal centers (GC), which are specialized, often transient, microstructures formed in the B cell follicles of secondary lymphoid tissues such as lymph nodes and spleen in response to infection or immunization (7–10). GC B cells exhibit unique spatiotemporal dynamics (11, 12). A GC is polarized, containing two distinct, physically separated zones: the dark zone (DZ) and the light zone (LZ). In the DZ, B cells undergo clonal proliferative bursts, during which somatic hypermutation (SHM) occurs. During SHM, the hypervariable regions of the genes encoding the immunoglobulin heavy chains and light chains are point-mutated by activation-induced cytidine deaminase (AID) at a high rate (13). As a result, the BCR affinities of the participating B cell clones for the invading antigen are modified and diversified. During SHM those B cells incurring damaging mutations that prevent normal assembly of surface BCRs are killed via apoptosis in the DZ (14, 15). After exiting the cell cycle following a proliferative burst, B cells migrate from the DZ to LZ under the chemoattractant force by CXCL13 secreted by follicular dendritic cells (FDCs) in the LZ (16, 17).

In the LZ, two main cell types participate in the positive selection of B cell clones harboring immunoglobulin (Ig) gene variants encoding relatively high-affinity antibodies: the residential FDCs and CD4<sup>+</sup> T follicular helper (Tfh) cells. These two cell types coordinate to provide key molecular signals for B cell activation, survival, DZ re-entry, proliferation, and differentiation (18–20). FDCs are antigen-presenting cells (APCs), which previously encountered and engulfed pathogens and present the antigen epitopes on their cell surface. When B cells first encounter FDCs, their BCRs are activated by the surface antigens of FDCs.

B cells then internalize the antigen-BCR complex and present the antigen epitopes on their own surface through major histocompatibility complex (MHC) II molecules to form peptide-MHCII complex (pMHCII). The density of pMHCII on the cell surface is proportional to the BCR affinity. Stronger BCR signaling also leads to higher PI3K-AKT-FOXO1 signal transduction (18, 21, 22). When the B cells subsequently encounter Tfh cells, a complex mutual interaction occurs between the two cell types (19, 23, 24). Tfh cells are activated via T cell receptors (TCR) liganded by pMHCII of the B cells, as well as by other cell surface signaling molecules such as inducible co-stimulator ligand (ICOSL) (25). Activated Tfh cells in turn express surface CD40L which reciprocally activates B cells together with several secretory cytokines including interleukins (IL) 4, 10, and 21 (26–28). CD40 signaling leads to NF-κB activation, increasing the chance of survival of B cells. In the presence of downregulated FOXO1, NF-κB elicits transient MYC activation that initiates the cell cycle (18). Only a small fraction of B cells is positively selected, which express CXCR4, the receptor for chemokine CXCL12, and migrate back to DZ where they undergo further proliferative bursts and SHM (16, 22). Those B cells with weaker BCR affinity are more likely to undergo apoptosis in the LZ, as well as B cells that do not have a chance to encounter Tfh cells in the LZ. As a result of combined action of proliferation and SHM in the DZ and positive selection in the LZ, the overall BCR affinity of the GC B cell population for the antigen continues to improve. After many rounds of DZ-LZ cycles, a small fraction of B cells are affinity-matured and exit the GC as either long-lived antibody-secreting PCs or memory B cells.

The GC plays a critical role in the generation of long-term protective immunity, and this is relevant in both the context of natural infection and vaccination for infectious diseases such as COVID-19 (29). If the GC is compromised or cannot be sufficiently induced due to genetic alterations, increased susceptibility to bacterial and viral infections will result. On the other hand, unintentional recognition of self-antigens and induction of GC can lead to autoimmune diseases such as systemic lupus erythematosus (30). Dysregulated B cell proliferation in GC can lead to lymphoma or other B cells-related leukemia (31). The GC also plays a role in antibody-mediated rejection of transplanted organs (32). In addition, many environmental contaminants are immunotoxicants, some of which can suppress B cell activation and the humoral immune response, leading to increased susceptibility to infectious disease and cancer (33). Therefore, a full mechanistic understanding of the complexity of GC is crucially important for sustaining immune integrity and preventing or alleviating many pathological conditions.

Computational modeling has played a long-standing role in dissecting and understanding the complex dynamics of GC immune responses (34, 35). The GC involves an elaborate interplay between many cell types, signaling molecules, transcription factors, and actuator genes (36). Key signal transduction and gene regulatory networks underpin the spatiotemporal dynamics of GC B cells and are crucial for the positive selection and ultimate formation of high-affinity PCs. Although there have been many efforts simulating the cellular dynamics and affinity maturation of GCs, cross-scale modeling that integrates molecular, cellular, and tissue-level

actions in a spatial context has only begun to emerge recently and thus is still rare (37–39). In this study, we presented a novel multiscale mathematical modeling framework of the GC developed in the CompuCell3D simulation environment that integrates the molecular network and spatiotemporal behaviors of GC B cells. The modeling framework provides an open-source, customizable, multiscale virtual GC platform that enables future *in silico* investigations of a range of questions both qualitatively and quantitatively, including B cell population turnover, BCR mutation rate, death timer, proliferative burst size, availability of Tfh cells, and effects of genetic and chemical perturbations.

## 2 Methods

### 2.1 Model structure

#### 2.1.1 Cell types, cellular events, and interactions modeled

Four major cell types involved in GCR are modeled in the framework: CXCL12-expressing reticular cells (CRCs) located in the DZ, FDCs and Tfh cells in the LZ, and B cells cycling between the DZ and LZ (7–10). For simplicity, CRC, FDC, and Tfh cells are treated as stationary. Key cellular events of B cells captured in the model include: (i) B cell volume growth, division, SHM, and apoptosis in the DZ; (ii) LZ-to-LZ B cell migration and simultaneous initiation of a cell death timer; (iii) interaction of B cells with FDCs in the LZ to determine BCR antigen affinity, interaction of B cells with Tfh cells in the LZ to make probabilistic decisions based on pMHCII density on positive

selection, survival, initiation of cell growth, and DZ re-entry of positively selected B cells, and death timer-triggered apoptosis of LZ B cells not positively selected.

#### 2.1.2 Molecular events in B cells

The above cellular events are driven by an intracellular molecular network in B cells that responds to diffusive chemoattractants and signaling molecules from FDCs and Tfh cells. For simplicity, the following molecular species and regulatory events are included in the model (Figure 1). A DZ-to-LZ descending gradient of chemoattractant CXCL12 is established by CRCs in the DZ (40, 41), and an opposite gradient of chemoattractant CXCL13 is established by FDCs in the LZ (17, 42). In the LZ, the contact of a B cell with an FDC will trigger BCR-mediated signal transduction, which leads to several signaling events in the modeled B cell: (i) re-expression on B cell surface of pMHCII, the density of which depends on BCR affinity for the antigen, (ii) transient activation of AKT and downregulation of FOXO1, the extent of which depends on BCR affinity (18, 21, 22), (iii) once the BCR affinity reaches a threshold, a switch-like activation of NF- $\kappa$ B subtype RelA is triggered (43–45), which in turn induces BLIMP1 (46, 47), leading to terminal B cell differentiation into antibody-secreting PCs.

If a B cell expressing pMHCII encounters a Tfh cell, the B cell is stimulated via CD40 signaling which activates another NF- $\kappa$ B subtype, cRel. cRel activation leads to at least two molecular signaling events. It activates Bcl-xL which inhibits apoptosis, thus terminating the death timer (48). With FOXO1 still downregulated, cRel also induces the expression of MYC (18). Upregulation of MYC triggers a commitment to cell growth and initiates the cell

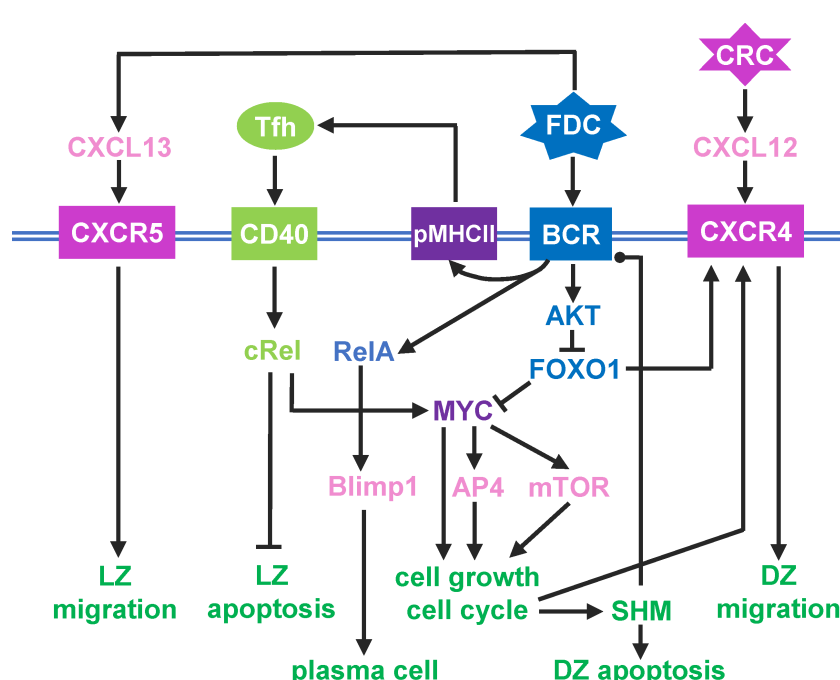


FIGURE 1

Schematic illustration of a simplified intracellular molecular network of GC B cells and different B cell outcomes driven by key molecules as indicated. Pointed arrowhead: stimulation/activation, blunted arrowhead: inhibition, and dotted arrow head: regulation in either direction.

cycle (49). MYC also activates AP4, which sustains B cell growth and division burst (50). With the B cell committed to growth and proliferation, as FOXO1 is re-expressed, CXCR4 is induced (22, 51). As a result, the B cell migrates towards the DZ in response to the CXCL12 gradient. In the DZ, shortly after each cell division, each of the two daughter cells incurs an independent point mutation of the BCR, which alters its affinity for the antigen with some probabilities (52–54). The probability of a damaging mutation is encoded such that a fraction of B cell progeny dies by apoptosis in the DZ (14, 15). The surviving B cells will continue to grow and divide as long as AP4 remains above a threshold (50). When AP4 drops below the threshold, the B cells exit the cell cycle, followed shortly by downregulation of CXCR4 (55). With CXCR5 constitutively expressed (12, 16), the B cells will be pulled by the CXCL13 gradient field into the LZ, repeating the DZ-LZ cycle.

### 2.1.3 Model assumptions and simplification

The molecular and cellular events involved in the GC are complex. Here, for the purpose of modeling, several assumptions and simplifications are made.

- i. The mutual activation between B cells and Tfh cells is simplified to pMHCII density-dependent CD40-cRel activation, as described above.
- ii. Many factors involved in GC, including BCL6, BACH2, and IRF4, are not explicitly considered.
- iii. Initial migration of B cells from the T/B cell border towards the LZ is not considered and neither is the Tfh cell migration into the LZ. CSR is thus not included as it is believed to occur primarily during pre-GC formation (56).
- iv. The initial clonal expansion of GC seeder B cells without SHM and positive selection is not considered for the lack of clear known mechanisms that terminate this initial proliferative burst phase and start the subsequent competitive selection phase.
- v. For B cells returning to the DZ, a delay variable is introduced before the cell growth for the first cell cycle is initiated to reduce the chance of cell division in the LZ.
- vi. The GC exit of PCs is modelled as deleting these cells from the simulation once they emerge.
- vii. Formation of memory B cells is not considered.

## 2.2 Construction of the computational model in CompuCell3D

The GC model was constructed and simulated as a hybrid, agent-based stochastic model in CompuCell3D. CompuCell3D provides a flexible and customizable platform for simulating multi-cellular behaviors and interactions based on the Glazier-Graner-Hogeweg approach (57). The Cellular Potts Model module in CompuCell3D was employed to simulate the physical properties and movements of individual B cells (58), while the

molecular network operating in each individual B cell, as depicted in Figure 1, was simulated by using the Gillespie's stochastic algorithm implemented in Tellurium conforming to the Antimony notation (59, 60). The CompuCell3D model consists of four files: an XML file, a Potts initialization file (PIF), and two Python script files. The XML file contains various “Plugins” and “Steppables” that define some default Potts model parameter values. The *Chemotaxis* plugin defines CXCL12 and CXCL13 as the chemoattractants, and the *DiffusionSolverFE* steppable designates that CXCL12 and CXCL13 are secreted by CRC and FDC, respectively and specifies the parameter values for secretion, diffusion, and decay in the Medium. The PIF file contains the initial coordinates of medium and cells where applicable. The steppable Python file contains the script that defines several steppable classes, including *GCR\_Stepable*, *MitosisStepable*, *BCell\_GRNStepable*, and *VisualizationStepable*, and the Tellurium model. The model is initialized in the “start” section of *GCR\_Stepable*, including the generation of CRCs, FDCs, Tfh cells, and seeding B cells. Each B cell is assigned a Tellurium molecular network model named as *BcellNetwork*.

### 2.2.1 Cell-cell contact and probabilistic decision-making

To capture the physical contact between B cells, FDCs, and Tfh cells, the *NeighborTracker* and *PixelTracker* plugins are employed to identify the neighboring cells of each B cell. Once a contact with an FDC is identified, the pMHCII level of the B cell is set proportional to its antigen-specific BCR affinity. Upon subsequent contact with a Tfh cell, the B cell can be positively selected based on a probability that is proportional to the pMHCII level. For the positively selected cell, the running death timer is terminated, cell cycle is committed, and DZ re-entry is initiated.

### 2.2.2 SHM and probability of BCR affinity alteration

Each of the two daughter cells of a dividing B cell has a probability of 0.3 to produce a damaging mutation that will result in cell death in the DZ. For the daughter cell that does not incur a damaging mutation, an SHM can either increase, decrease, or does not change the BCR affinity, each with a probability of 1/3. The increment or decrement of the affinity alteration can be either 0.25 or 0.5 with equal probability. In general, the BCR affinity ranges between 0–10, but can be higher.

## 2.3 Simulation data collection, storage, analysis, and model sharing

Variables of each B cell are saved in a plain text file which is updated every 15 Monte Carlo steps (*mcs*). The file is named in the format of “Generation\_mother ID\_cell ID.txt” to facilitate lineage tree construction. The CompuCell3D model files containing the parameter values and Python script for analysis of simulated data are available at <https://github.com/pulsatility/2024-GCR-Model.git>.

### 3 Results

#### 3.1 Morphology of a simulated GC

The morphological results of a representative simulation of the GC model are shown in **Figure 2**. The simulated space dimension is 250x200x11 pixels, which can be considered as 250x200x11 in  $\mu\text{m}$  in real space, to represent a slice of the GC to save computational time. The 2-D projection of the instantiated non-B cells on the X-Y

plane is indicated in **Figure 2A**, while along the Z dimension, these cells are distributed randomly in 3 of the 11 layers (results not shown). There are 45 CRCs distributed on the left half of the field, which becomes the future DZ, and 45 FDCs and 36 Tfh cells distributed on the right half of the field, which becomes the future LZ. Tfh cells are located next to FDCs, reflecting the notion that they also express CXCR5 and are thus drawn to FDCs which secrete chemoattractant CXCL13 (61, 62). Not all FDCs are surrounded by Tfh cells, mimicking the situation that the availability of Tfh cells is

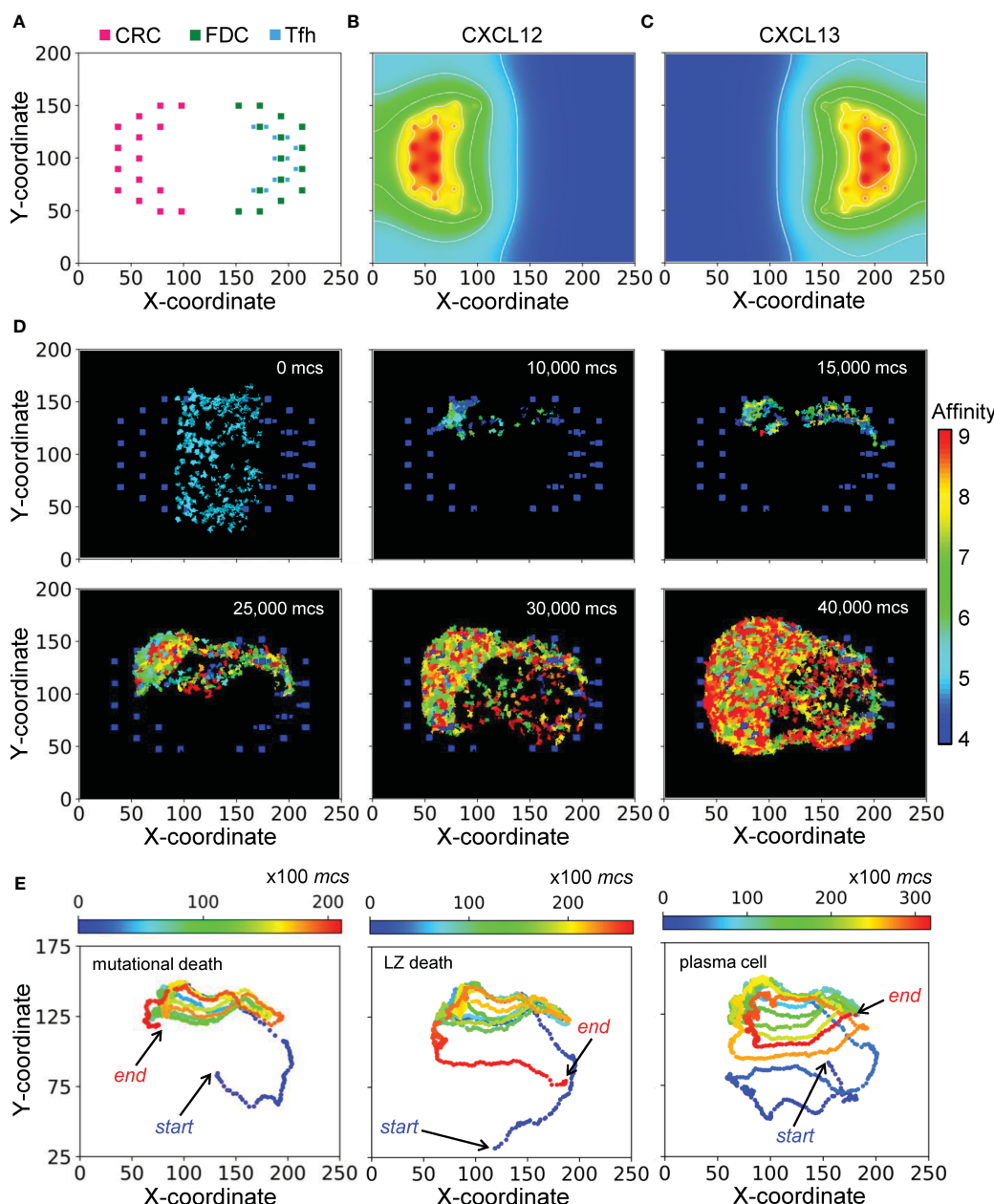


**FIGURE 2**

Morphology of a representative simulated GC. **(A)** 2-D distributions of CRCs, FDCs, and Tfh cells in the DZ (left) and LZ (right) with X-Y coordinates indicated. **(B, C)** Concentration gradients of chemoattractants CXCL12 and CXCL13 respectively. White contour lines: isolines of equal concentrations. **(D)** Snapshots of simulated GC at various  $mcs$  indicated. Colors of B cells denote BCR/antibody affinity as indicated by the colormap. **(E)** 2-D trajectories of B cells in three select lineages leading respectively to damaging mutation-induced apoptosis in DZ (left panel), death timer-triggered apoptosis in the LZ for not positively selected (mid panel), and emergence of a PC (right panel). Dot color denotes  $mcs$  time as indicated by the colormap.

a limiting factor in the positive selection of LZ B cells (12, 63–65). CRCs and FDCs secrete CXCL12 and CXCL13 respectively, establishing two opposing chemoattractant fields and thus the polarity of the GC (Figures 2B, C).

With the layout of residential cells and chemoattractant fields as above, a simulated GC that succeeds in producing B cells of high BCR/antibody affinities is shown as snapshots in Figure 2D and in Supplementary Video S1. For this simulation, the GC starts with 200 B cells (clones) of intermediate affinity of 5 (indicated by the color of the cells) between the DZ and LZ. Over a period of 40,000 Monte Carlo steps (*mcs*, where 100 *mcs* can be regarded approximately as 1 hour in real time), both the number of total GC B cells and the fraction of high-affinity B cells increase, indicating successful GC population growth and affinity maturation. The 2-D trajectories of 3 select B cell lineage branches leading to different cell fates are shown in Figure 2E. These trajectories cycle between the DZ and LZ for multiple rounds. The first trajectory ends with cell death in the DZ due to damaging mutation during mitosis (left panel), the second trajectory also ends with cell death but in the LZ due to death timer (mid panel), and the last trajectory ends with differentiation into a PC in the LZ (right panel).

## 3.2 Cellular events of GC B cells

### 3.2.1 B cell population dynamics

In this section we performed an in-depth quantitative analysis of the GC B cell population dynamics with respect to time, location, and cell fates. For the GC simulation presented in Figure 2, the total number of B cells ( $N_{Tot}$ ) increases rapidly from the initial 200 over a period of 40,000 *mcs*, then approaches a steady-state size of about 2,500 cells through 72,000 *mcs* (equivalent to 30 days) without considering GC termination (Figure 3A). The growth of the B cell population is not smooth – it proceeds in an uneven fashion due to random births and deaths occurring simultaneously. In the early stage of the GC, the numbers of B cells in the DZ ( $N_{DZ}$ ) and LZ ( $N_{LZ}$ ) alternate in anti-phase, resulting from cyclic cell migration in unison between the two zones (Video S1). In the late stage,  $N_{DZ}$  is persistently greater than  $N_{LZ}$  with the  $N_{DZ}:N_{LZ}$  ratio stabilizing near 3:1 (Figure 3A). The evolving B cell population in the GC is highly dynamic with constant turnover through several processes. Specifically, (i) B cells are born in the DZ as a result of proliferative bursts of clonal expansion; (ii) B cells are cleared from the GC via apoptosis triggered by damaging BCR mutations in the DZ and via apoptosis in the LZ if not positively selected; and (iii) B cells exit the GC as PCs. We next quantified the birth and death (apoptosis) events.

#### 3.2.1.1 B cell birth

The number of B cells engaged in cell cycle increases over time and these cells are predominantly in the DZ (Figure 3B). There are a small number of cell cycle-engaged B cells in the LZ, representing positively selected B cells that just initiate the cell cycle without much growing yet. Approaching the steady state, nearly 70% and

30% of DZ and LZ B cells, respectively, are engaged in the cell cycle, while on average 65% of the overall B cell population is in the cell cycle (Figure 3C). B cells are born predominantly in the DZ with only a negligible number of births in the LZ (Figure 3D). The absolute birth rate increases over time approaching about 1100 births per 600 *mcs* (Figure 3E). Cumulative births reach 150K in the entire 72,000 *mcs* period when two birth events are registered for each cell division (Figure 3F). The mean cell generation increases almost linearly with time while the variability also progressively increases as more B cells are born (Figure 3G). The DZ B cell volumes exhibit a biphasic distribution, reflecting that these cells are actively engaged in growth and division (Figure 3H). In contrast, the LZ B cells exhibit a very narrow volume distribution consistent with the notion that they are mostly non-proliferating centrocytes.

#### 3.2.1.2 B cell death

As the GC B cell population grows, the number of cell deaths increases and then approaches a steady state, where the total death rate is about 1000 deaths per 600 *mcs* (Figure 3I). Although at the early time the DZ: LZ death rate ratio fluctuates dramatically as a result of randomness due to small numbers of cell deaths and DZ-LZ migration, the ratio stabilizes at about 2.5:1 at later time. The steady-state death turnover rate of the overall B cell population is slightly above 40% in 600 *mcs*, and the turnover rates in both zones are similar (Figure 3J). Cumulatively, there are nearly 70,000 cell deaths, among which 70% occurred in the DZ and 30% in the LZ (Figure 3K).

Further analysis showed that different types of cell deaths occur at different rates (Figure 3L). B cell death due to damaging BCR mutations occurs most often, comprising 65% of total deaths at steady state, followed by cell death due to no access to Tfh cells at 30%, while cell death for not being positively selected even after contacting Tfh cells (labelled as Neg selected) is only a small fraction of all death events (Figure 3M). When a B cell cannot access Tfh cells, positive selection decisions cannot be made in time and the B cell will die when the default death timer goes off. This type of death is only limited to B cells in the LZ initially, but as the GC population grows such that the space becomes more compact and thus crowded, such death also expands to the DZ when some of the B cells exiting the cell cycle do not have enough time to migrate through the densely populated DZ (Figure 3N); however, these deaths in the DZ are only a small fraction (Figure 3O).

### 3.2.2 Affinity maturation and clonal dominance

We next characterized the evolution of the BCR antigen affinities in the simulated GC. With all the 200 seeder B cells starting with an intermediate BCR affinity of 5 in this simulation, their clonal affinities initially drift to both higher and lower levels (Figure 4A). However, the mean affinity increases progressively in a winding manner and then reaches a plateau at about 8.5. The variabilities of the BCR affinities, as defined by the 25–75% quantiles and 2.5–97.5% percentiles, also shift upward and then plateau along with the mean, despite that the affinities of some B cells reach as low as near 2 and as high as over 12 at times. PCs start to emerge shortly after 20,000 *mcs*, with >10 affinity levels (Figure 4A, 10 is defined as

```

<CompuCell3D Revision="20210612" Version="4.2.5">

<Potts>
  <Dimensions x="250" y="200" z="11"/>
  <Steps>72000</Steps>
  <Temperature>15.0</Temperature>
  <NeighborOrder>1</NeighborOrder>
</Potts>

<Plugin Name="CellType">

  <!-- Listing all cell types in the simulation -->
  <CellType TypeId="0" TypeName="Medium"/>
  <CellType TypeId="1" TypeName="BCell"/>
  <CellType TypeId="2" TypeName="FDC" Freeze="" />
  <CellType TypeId="3" TypeName="CRC" Freeze="" />
  <CellType TypeId="4" TypeName="TCell" Freeze="" />
  <CellType TypeId="5" TypeName="Wall" Freeze="" />
</Plugin>

<Plugin Name="Contact">

  <Energy Type1="Medium" Type2="Medium">0.0</Energy>
  <!-- <Energy Type1="Medium" Type2="BCell">8.0</Energy> -->
  <Energy Type1="Medium" Type2="BCell">2.0</Energy>
  <!-- <Energy Type1="BCell" Type2="BCell">40.0</Energy> -->
  <Energy Type1="BCell" Type2="BCell">5.0</Energy>
  <!--<NeighborOrder>4</NeighborOrder-->
  <Energy Type1="FDC" Type2="FDC">0</Energy>
  <Energy Type1="FDC" Type2="Medium">0</Energy>
  <!-- <Energy Type1="FDC" Type2="BCell">50.0</Energy> -->
  <Energy Type1="FDC" Type2="BCell">3.0</Energy>
  <Energy Type1="CRC" Type2="FDC">0</Energy>
  <Energy Type1="CRC" Type2="Medium">0</Energy>
  <Energy Type1="CRC" Type2="BCell">3.0</Energy>
  <Energy Type1="CRC" Type2="CRC">0</Energy>
  <Energy Type1="TCell" Type2="FDC">0</Energy>
  <Energy Type1="TCell" Type2="Medium">0</Energy>
  <!-- <Energy Type1="TCell" Type2="BCell">8.0</Energy> -->
  <Energy Type1="TCell" Type2="BCell">3.0</Energy>
  <Energy Type1="TCell" Type2="CRC">0</Energy>
  <Energy Type1="TCell" Type2="TCell">0</Energy>
  <Energy Type1="Wall" Type2="FDC">0</Energy>
  <Energy Type1="Wall" Type2="Medium">0</Energy>
  <Energy Type1="Wall" Type2="BCell">30.0</Energy>
  <Energy Type1="Wall" Type2="CRC">0</Energy>
  <Energy Type1="Wall" Type2="TCell">0</Energy>
  <Energy Type1="Wall" Type2="Wall">0</Energy>
  <Depth>2</Depth>
</Plugin>

<Plugin Name="Chemotaxis">
  <ChemicalField Name="CXCL12"/>
  <ChemicalField Name="CXCL13"/>
</Plugin>

<Steppable Type="DiffusionSolverFE">
  <!-- <Steppable Type="SteadyStateDiffusionSolver"> -->
  <DiffusionField Name="CXCL13">
    <DiffusionData>
      <FieldName>CXCL13</FieldName>
      <DiffusionConstant>2</DiffusionConstant>

```

```
<DecayConstant>0.001</DecayConstant>
</DiffusionData>
<SecretionData>
    <Secretion Type="FDC">3.6</Secretion>
</SecretionData>
</DiffusionField>

<DiffusionField Name="CXCL12">
    <DiffusionData>
        <FieldName>CXCL12</FieldName>
        <DiffusionConstant>2</DiffusionConstant>
        <DecayConstant>0.001</DecayConstant>
    </DiffusionData>
    <SecretionData>
        <Secretion Type="CRC">3.6</Secretion>
    </SecretionData>
</DiffusionField>
</Steppable>

</CompuCell3D>
```